

The Pluripotency Factor-Bound Intron 1 of *Xist* Is Dispensable for X Chromosome Inactivation and Reactivation In Vitro and In Vivo

Alissa Minkovsky,^{1,2} Tahsin Stefan Barakat,³ Nadia Sellami,^{1,2} Mark Henry Chin,^{1,2} Nilhan Gunhanlar,³ Joost Gribnau,³ and Kathrin Plath^{1,2,*}

¹Department of Biological Chemistry, David Geffen School of Medicine, Jonsson Comprehensive Cancer Center, Molecular Biology Institute

²Eli and Edythe Broad Center of Regenerative Medicine and Stem Cell Research

University of California, Los Angeles, Los Angeles, CA 90095, USA

³Department of Reproduction and Development, Erasmus MC, University Medical Center, 3015 Rotterdam, The Netherlands

*Correspondence: kplath@mednet.ucla.edu

<http://dx.doi.org/10.1016/j.celrep.2013.02.018>

SUMMARY

X chromosome inactivation (XCI) is a dynamically regulated developmental process with inactivation and reactivation accompanying the loss and gain of pluripotency, respectively. A functional relationship between pluripotency and lack of XCI has been suggested, whereby pluripotency transcription factors repress the master regulator of XCI, the noncoding transcript *Xist*, by binding to its first intron (intron 1). To test this model, we have generated intron 1 mutant embryonic stem cells (ESCs) and two independent mouse models. We found that *Xist*'s repression in ESCs, its transcriptional upregulation upon differentiation, and its silencing upon reprogramming to pluripotency are not dependent on intron 1. Although we observed subtle effects of intron 1 deletion on the randomness of XCI and in the absence of the antisense transcript *Tsix* in differentiating ESCs, these have little relevance in vivo because mutant mice do not deviate from Mendelian ratios of allele transmission. Altogether, our findings demonstrate that intron 1 is dispensable for the developmental dynamics of *Xist* expression.

INTRODUCTION

To balance the expression of X-linked genes between males and females, female mammals silence one of the two X chromosomes in a developmentally regulated process called X chromosome inactivation (XCI). XCI occurs in two waves in the course of mouse embryogenesis. The earliest form of XCI begins at the two- to four-cell stage in preimplantation embryo and is imprinted, selectively occurring on the paternally inherited X chromosome (Xp) (Huynh and Lee, 2003; Kalantry et al., 2009; Namekawa et al., 2010; Patrat et al., 2009). At the preimplantation blastocyst stage, imprinted XCI is retained in the trophoblast and primitive endoderm lineages but reversed in arising pluripotent epiblast cells yielding a state with two active

X chromosomes (XaXa) (Mak et al., 2004; Okamoto et al., 2004; Silva et al., 2009; Williams et al., 2011). Upon implantation, these epiblast cells establish a random form of XCI that stochastically initiates on the maternal or paternal X chromosome and is retained through the lifetime of mitotic divisions (Kay et al., 1993; Rastan and Robertson, 1985). Similarly, mouse embryonic stem cells (ESCs), which are derived from epiblast cells of the preimplantation blastocyst, undergo random XCI when induced to differentiate ex vivo. The only exception to somatic maintenance of random XCI is inactive X (Xi) reactivation in the germline, which is assumed to be essential for female fertility and occurs in primordial germ cells as they traverse the hindgut to seed the genital ridges (Chuva de Sousa Lopes et al., 2008; de Napoles et al., 2007; Sugimoto and Abe, 2007). Xi reactivation is also a feature of experimentally induced acquisition of pluripotency via transcription factor-mediated reprogramming to induced pluripotent stem cells (iPSCs), fusion of somatic cells with ESCs, or somatic cell nuclear transfer (Eggan et al., 2000; Maherali et al., 2007; Tada et al., 2001).

The cycles of XCI and Xi reactivation are associated with changes in *Xist* RNA coating, where cells with a Xi display coating by the noncoding *Xist* RNA on the Xi chromosome, and those with two active X chromosomes lack *Xist* RNA expression (Brockdorff et al., 1991; Brown et al., 1991). *Xist*'s function has been most studied in the random form of XCI in the mouse system, where it is shown to be the critical trigger of XCI. The upregulation of *Xist* RNA and coating of the X at the onset of random XCI immediately lead to transcriptional silencing of X-linked genes and result in the exclusion of RNA polymerase II and the recruitment of repressive chromatin-modifying protein complexes such as the Polycomb complex PRC2, which establishes an accumulation of H3K27me3 (Chaumeil et al., 2006; Chow and Heard, 2009; Plath et al., 2003; Silva et al., 2003). A stereotypic order of changes in chromatin structure culminates in heritable silencing of either the maternally or paternally transmitted X chromosome in each cell of the female adult mammal. *Xist* is essential for XCI to occur in cis because its deletion leads to silencing of the other X chromosome carrying an intact *Xist* allele, regardless of parent of origin (Marahrens et al., 1997; Penny et al., 1996). Moreover, the importance of *Xist* regulation for the developmental and sex-specific context of XCI is

demonstrated by its sufficiency: overexpression of a X-linked *Xist* cDNA transgene in male mouse ESCs (XY:tetOP-*Xist*) initiates XCI and cell death due to silencing of the single X chromosome (Wutz and Jaenisch, 2000).

Xist is transcribed from a larger locus on the X chromosome that has been defined as the minimal critical region for XCI and besides housing *Xist*, contains other protein-coding and non-coding activators and repressors of *Xist*, some of which act in *cis* and others in *trans* (Rastan and Robertson, 1985; reviewed in Minkovsky et al., 2012). The best-characterized repressor of *Xist* is its antisense transcript, *Tsix*, which is highly transcribed in epiblast cells of the preimplantation blastocyst and in undifferentiated mouse ESCs/iPSCs, where *Xist* is repressed (Lee et al., 1999; Sado et al., 2001; Maherali et al., 2007). Deletion of *Tsix* leads to only slight *Xist* upregulation without causing precocious XCI or *Xist* RNA coating in self-renewing, undifferentiated ESCs. However, upon differentiation, XCI is skewed to the *Tsix*-deleted X in female cells heterozygous for the mutant *Tsix* allele (Lee et al., 1999; Lee, 2000; Luikenhuis et al., 2001; Sado et al., 2001). The effect of *Tsix* deletion on *Xist* indicates that it participates in parallel pathways with other regulators of *Xist* repression or activation.

Interestingly, the pluripotency factors Oct4, Sox2, and Nanog have been implicated in the control of *Xist* expression in pluripotent cells. Navarro and colleagues found that in mouse ESCs, Oct4, Sox2, and Nanog bind the first intron of the *Xist* gene (intron 1) (Navarro et al., 2008), a finding that has been recapitulated in many genomic data sets and extends to additional pluripotency regulators such as Tcf3 and Prdm14, and early developmental regulators such as Cdx2 (Figure S1A; Loh et al., 2006; Marson et al., 2008; Ma et al., 2011; Erwin et al., 2012). Such genomic regions of extensive pluripotency transcription factor co-occupancy in the ESC genome occur more commonly than would be expected by chance (Chen et al., 2008). It is thought that these cobound genomic regions represent functionally important sites and often represent enhancer elements (Chen et al., 2008). Further support for a gene regulatory role of intron 1 is that, in ESCs, the intron 1 region has a propensity to be in the three-dimensional proximity to the promoter of *Xist* and adopts a DNase hypersensitive state (Tsai et al., 2008). Additionally, pluripotency factors appear directly linked to *Xist* regulation. Upon *Nanog* deletion or inducible repression of *Oct4*, *Xist* is upregulated, and binding of the pluripotency factors to intron 1 is lost (Navarro et al., 2008). In male ESCs, which normally do not upregulate *Xist*, experimentally forced *Oct4* repression can even induce *Xist* RNA coating in up to 10% of the cells (Navarro et al., 2008). Another study could not replicate *Xist* RNA coating upon *Oct4* knockdown in male ESCs but observed biallelic XCI in differentiating female ESCs upon *Oct4* depletion (Donohoe et al., 2009). A role for Nanog in *Xist* suppression is also supported by its expression pattern with regard to domains of Xi reactivation in the preimplantation blastocyst, where the restriction of Nanog expression demarcates the fraction of cells undergoing reactivation of the imprinted Xi (Silva et al., 2009). Furthermore, preimplantation embryos lacking Nanog are unable to specify epiblast cells and to lose *Xist* RNA, whereas forced expression of Nanog induces a more rapid loss of *Xist*

RNA coating in developing preimplantation embryos (Silva et al., 2009; Williams et al., 2011).

Together, these findings led to the model that pluripotency factor binding to intron 1 is critical for repression of *Xist* in undifferentiated XaXa ESCs. However, in the experiments leading to this conclusion, cell identity and, therefore, likely the expression of many genes were modulated by experimental changes in pluripotency factor expression, which could confound the interpretation that Oct4, Nanog, and other pluripotency factors act directly on intron 1 of *Xist* to regulate XCI. It has also been suggested that the pluripotency transcription factors control the levels of positive and negative regulators of *Xist* because they are binding to *Tsix* and the *trans*-acting activator of XCI, *Rnf12* (Donohoe et al., 2009; Gontan et al., 2012; Navarro et al., 2010, 2011). Accordingly, an experiment directly addressing the functional importance of binding to intron 1 showed only subtle dysregulation of XCI: in female ESCs carrying a heterozygous deletion of intron 1 of *Xist*, XCI remained suppressed in the undifferentiated state. However, upon differentiation, *Xist* appeared more highly expressed from the chromosome carrying the mutation, supporting a role for intron 1 in suppressing *Xist* during differentiation (Barakat et al., 2011). Furthermore, deletion of intron 1 in the context of a transgene carrying the extended *Xist* locus moderately increased expression of *Xist* in undifferentiated ESCs, which was amplified by simultaneous deletion of the antisense transcript *Tsix* (Nesterova et al., 2011). Notably, these results were very variable between clones potentially reflecting the effect of transgene copy number and variations (Nesterova et al., 2011). Binding to *Xist* intron 1 has also been proposed to govern the switch from imprinted to random XCI in preimplantation development (Erwin et al., 2012). In vitro, gel shift assays suggest that the binding events between *Xist*'s intron 1 and the pluripotency regulator Oct4 and the trophectoderm regulator Cdx2 are direct but mutually exclusive (Erwin et al., 2012). Collectively, these findings motivated us to examine the role of *Xist* intron 1 further to test the model wherein pluripotency factor binding silences *Xist* to prevent XCI in pluripotent cells and to determine the role of the intronic region in X chromosome reactivation events, both in vivo and in vitro.

RESULTS

Generation of Conditional *Xist* Intron 1 ESC Lines

To further define the role of *Xist* intron 1, we used gene targeting to generate a conditional allele in male and female mouse ESCs. We tested the requirement of intron 1 in both sexes because male ESCs are able to undergo XCI upon forced expression of *Xist*, providing a sensitive background for monitoring *Xist* regulation independently of other X chromosomes present in a cell (Wutz and Jaenisch, 2000). By contrast, heterozygous female ESCs permit investigation of kinetics of XCI upon induction of differentiation and insight into potential effects on skewing of XCI between the targeted and wild-type (WT) chromosome.

To delineate the region of intron 1 involved in *Xist* repression, we inspected where pluripotency transcription factors bind within the intron 1 region as detected by published chromatin immunoprecipitation sequencing (ChIP-seq) data sets (Marson et al., 2008). We also determined the localization of pluripotency

factor DNA binding motifs and considered sequence conservation across mammals (Figure S1). We found that co-occupancy of pluripotency factors occurs in a 600 bp region within the full 2.8 kb sequence of intron 1. Most of the intron 1 sequence is not conserved in placental mammals; however, two highly conserved composite Oct4-Sox2 DNA binding motifs, which are found to stabilize a ternary Oct4-Sox2-DNA complex in the expression of many ESC-specific genes, underlie the ChIP-seq binding peaks of Oct4 and Sox2 (Figure S1; Reményi et al., 2003; Marson et al., 2008; Mason et al., 2010; UCSC genome browser phastCons conserved-elements track, <http://genome.ucsc.edu>). On the basis of these data, we decided to delete 800 bp of intron 1 and, subsequently, refer to this mutation as “intron 1” (Minkovsky/Plath allele; Figure S1).

We flanked the 800 bp intron 1 region with loxP sites, simultaneously inserting a hygromycin-resistance cassette (yielding a targeted allele with 3loxP sites), and, subsequently, generated experimental (1lox) and control (2lox) alleles by transient expression of Cre recombinase in hemizygotously targeted male and heterozygous female ESCs (Figures 1 and S2). To be able to monitor the effects of the deletion of intron 1 on *Xist* in cis in female cells, we employed genetically polymorphic F1 2-1 female ESCs (129/Cas) carrying a MS2 RNA tag in exon 7 of *Xist* on the 129 allele (Jonkers et al., 2008). Southern blotting and PCR analysis confirmed that intron 1 was targeted in cis to the MS2 RNA tag in female ESCs (Figure S2). Male- and female-targeted ESC lines showed normal chromosome complement upon karyotyping (Figure S2; data not shown).

To confirm that deletion of 800 nucleotides from intron 1 sufficiently removes pluripotency factor binding, we performed ChIP against Oct4 and Sox2 coupled to quantitative PCR for the targeted region of intron 1, neighboring intronic regions, the *Xist* promoter, and previously validated control regions (Navarro et al., 2008). Importantly, we did not observe an increase in Oct4 or Sox2 binding in these regions upon deletion of intron 1 (Figures 1G–1I). Thus, compensatory binding at cryptic binding sites upon intron 1 deletion appears unlikely.

Ectopic *Xist* RNA Coating Is Not Observed in Intron 1-Deleted Undifferentiated and Differentiating Male and Female ESCs

To understand the role of intron 1 in the regulation of XCI, we first performed fluorescence in situ hybridization (FISH) to analyze the expression and localization of *Xist* and *Tsix* RNA at the single-cell level using strand-specific RNA probes. Undifferentiated male and female ESC lines displayed no significant *Xist* RNA cloud or pinpoint signal in the presence or absence of intron 1 (Figures 2A and 2B). The absence of *Xist* RNA coating in the undifferentiated ESC state was confirmed by the lack of a Xi-like enrichment of H3K27me3 in Nanog⁺ cells, which is known to occur on the Xi when *Xist* RNA coats (Plath et al., 2003; Silva et al., 2003) (Figures S3A and S3B). In agreement with this finding, the signal for *Tsix* was present in the majority of cells in each case and indistinguishable among all tested genotypes (Figure 2A).

Upon induction of differentiation by embryoid body (EB) formation, the lack of intron 1 did not induce *Xist* RNA in male ESCs to a level detectable by FISH (data not shown) and yielded

no Xi-like enrichment of H3K27me3 (Figures S3C and S3D), indicating that intron 1 is not an essential regulator of *Xist* suppression in differentiating male ESCs when all other regulators of XCI are intact. Heterozygous 1lox/WT female ESCs formed *Xist* RNA clouds and H3K27me3 Xi foci at comparable rates to 2lox/WT control ESCs (Figures 2C, 2D, S3C, and S3D). *Xist* RNA levels were also similar between undifferentiated and differentiating male and female ESCs, with or without intron 1, in RT-PCR experiments (Figure 2E). Proper differentiation was confirmed by decrease in *Nanog* transcript levels (Figure 2F). Furthermore, the use of *Xist* intron 1-spanning PCR primer pairs ruled out dramatic secondary effects of intron 1 deletion on *Xist* splicing (data not shown).

Next, we assessed whether XCI is skewed upon intron 1 deletion in differentiating female ESCs. The polymorphic 129/cas F1 2-1 female ESC line is known to have a baseline skewing of XCI toward the 129 allele such that approximately 70% of the cells will silence the 129 allele, due to strain-specific haplotypes (Cattanach and Isaacson, 1967). Due to the integration of the MS2 RNA tag on the intron-targeted 129 X chromosome, combined RNA-FISH for MS2 and *Xist* sequences can distinguish between *Xist* being expressed from the targeted chromosome (positive for both *Xist* and MS2 signals) and the untargeted X (only marked by the *Xist* probe) (Figure 2C; Jonkers et al., 2008). We found that, at the single-cell level, female 1lox intron/WT ESCs consistently had ~15% more cells expressing the MS2-tagged *Xist* than their 2lox/WT counterparts, in three of four ex vivo differentiation methods (Figures 2G and S4). This mild skewing effect in differentiating female ESCs is consistent with published results (Barakat et al., 2011).

Genetic Interaction of *Xist* Intron 1 with *Tsix*

Next, we investigated the possibility that the intron 1-dependent skewing of XCI in differentiating female ESCs represents a mild effect on the intron 1-deleted X chromosome at the transition to the differentiated state. We reasoned that such an effect may be more strongly revealed in the absence of other regulators of *Xist* and sought to assay such an effect on a “sensitized” background for *Xist* transcription. *Tsix* represents the prime candidate for a redundant *Xist* repressor that could compensate to repress *Xist* in the absence of intron 1. One study supports the view that a functional role for the intron can be uncovered in the absence of *Tsix* because male ESCs with randomly integrated genomic *Xist* transgenes lacking intron 1 and a functional *Tsix* allele dysregulated the expression of the transgenic *Xist* (Nesterova et al., 2011). We therefore performed the aforementioned analyses in male ESCs lacking intron 1 in the endogenous *Xist* allele on the background of a previously characterized *Tsix* loss-of-function mutation at the endogenous locus (Figure 3; Lee et al., 1999; Luikenhuis et al., 2001; Sado et al., 2001). We targeted the disruption of *Tsix* to both 2lox and 1lox intron male ESCs using a construct that inserts a splice acceptor-IRES β Geo cassette in exon 2 of *Tsix* resulting in an early transcriptional stop (Figure 3A) (Sado et al., 2002). Correct targeting and loss of the *Tsix* transcript were confirmed by Southern blot (Figure 3B) and absence of FISH signal for *Tsix* (Figure 3C).

As expected, in the presence of intron 1 (2lox intron 1), *Tsix* deletion in male ESCs induced a mild transcriptional

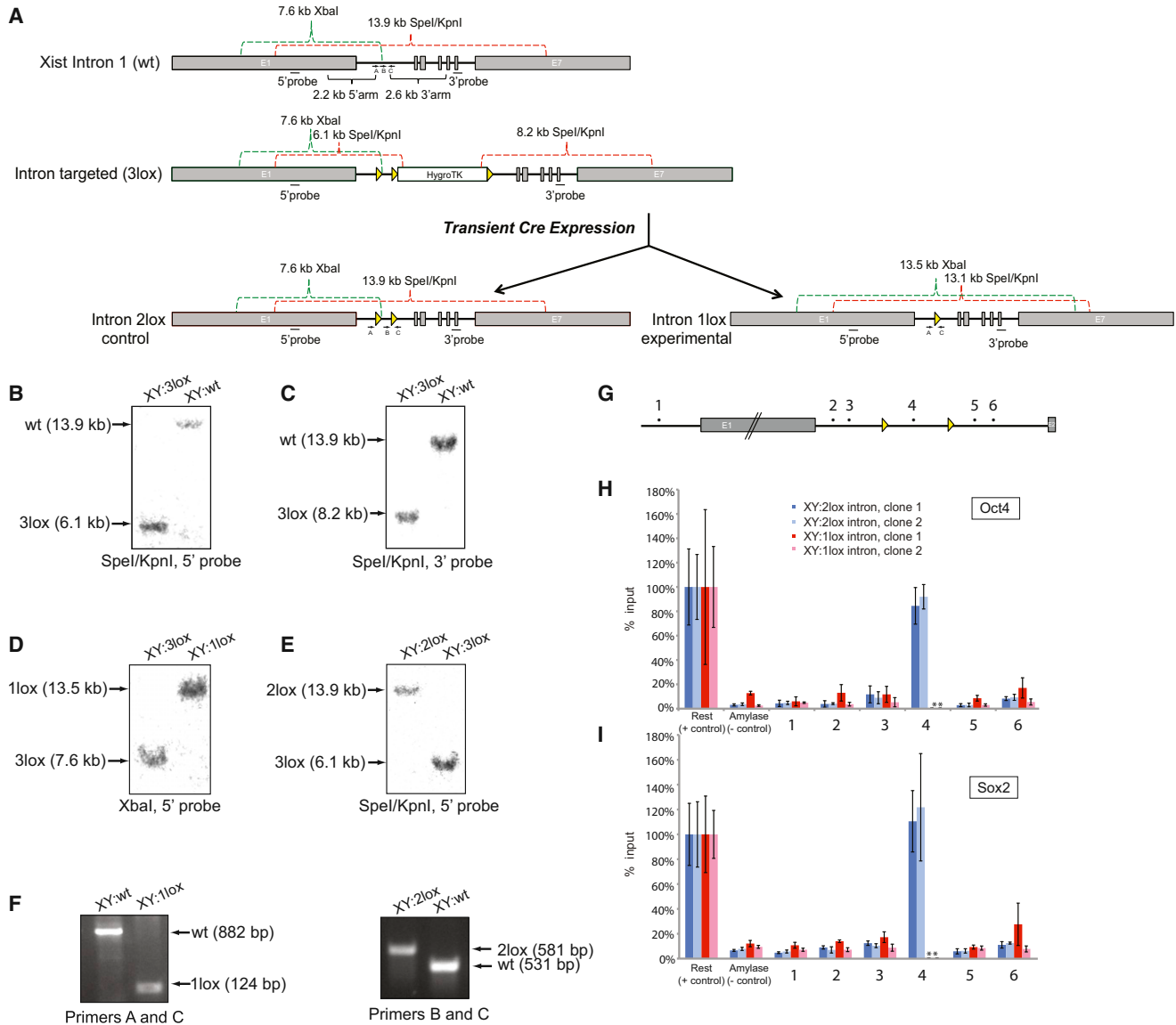


Figure 1. Generation of Male mouse ESCs Carrying a Conditional *Xist* Intron 1 Allele

(A) Gene targeting and Southern blotting strategy schematic for male ESCs. Transient expression of Cre recombinase in properly targeted 3lox clones yielded both 2lox (control) and 1lox (experimental) ESC lines.

(B–E) Representative images of correctly targeted clones from Southern blot analysis.

(F) PCR genotyping with primers A and C shows the presence of the 1lox allele, and genotyping with primers B and C shows that of the 2lox allele.

(G) Location of ChIP-qPCR primer sets within the *Xist* locus used in the subsequent figures. Primer pair 1 is located within the *Xist* promoter.

(H and I) ChIP-qPCR analysis of Oct4 (H) and Sox2 (I) binding to regions indicated in (G) and a known positive and negative control (within Rest and Amylase, respectively) for Oct4 and Sox2 binding (van den Berg et al., 2008) in 2lox and 1lox intron 1 male ESCs (two clones each). Values represent the amount of DNA precipitated after normalization to input chromatin and are given relative to binding within the positive control region. Error bars represent SD from triplicate qPCR measurements. Asterisk (*) indicates high Ct values for the input samples in the genetically deleted regions, probably arising from support feeder cells.

See also Figures S1 and S2.

upregulation of *Xist* RNA compared to XY:2lox/*Tsix*-WT ESCs in RT-PCR experiments, reaching a level found in female ESCs (Figure 3D). Upon differentiation, XY:2lox intron/*Tsix*-Stop ESCs further upregulated *Xist* transcript levels ~5-fold (Figure 3D). However, this induction was rarely correlated with a *Xist* RNA cloud signal detectable by RNA FISH or a Xi-like

H3K27me3 accumulation (Figures 3E–3H) before and after induction of differentiation, in agreement with previous reports by Luikenhuis et al. (2001) and Sado et al. (2002). Combined deletion of intron 1 and *Tsix* did not alter the *Xist* status in undifferentiated ESCs but upon induction of differentiation, resulted in a *Xist* RNA cloud-like signal in FISH experiments in 3%–6% of

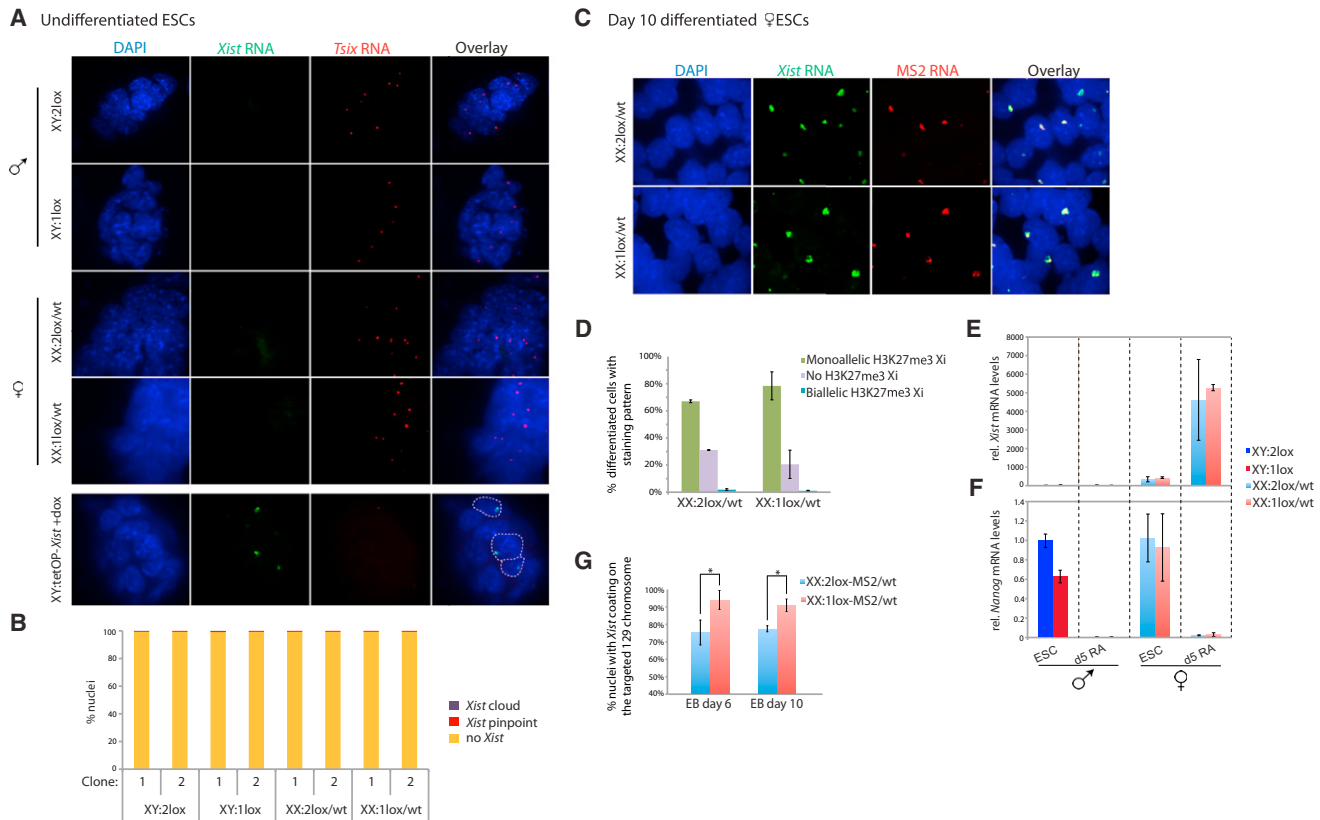


Figure 2. Analysis of *Xist* Expression in Undifferentiated and Differentiating Female and Male ESC Lines in the Presence and Absence of Intron 1

(A) Strand-specific FISH for *Xist* RNA (green) and *Tsix* RNA (red) in undifferentiated male and female ESCs of the indicated genotypes, using RNA probes. DAPI staining (blue) indicates nuclei. Representative images are shown. A male ESC line carrying a doxycycline (dox)-inducible *Xist* allele in the endogenous locus was used as positive control for the *Xist*-staining pattern, at 24 hr of dox addition.

(B) Graph summarizes the proportion of DAPI-stained nuclei with indicated patterns of *Xist* RNA based on an experiment as described in (A). Pairs of independent ESC clones of the given genotype were stained and counted. In each case, 500 nuclei were assessed.

(C) FISH with DNA probes targeting *Xist* RNA (green) and the *MS2* tag (red), respectively, in female ESCs of indicated genotypes at day 10 of EB differentiation.

(D) Graph summarizing the proportion of Nanog-negative cells in day 10 EB-differentiated female ESCs with no, one, or two H3K27me3 Xi-like accumulations. Notably, the number of cells within each H3K27me3 pattern is not statistically different (by Student's t test) between 2lox/wt and 1lox/wt ESC lines. Values are means of counts of independent clones as shown in Figure S4D; in each case, at least 500 nuclei were assessed.

(E) RT-PCR for *Xist* RNA levels normalized to *Gapdh* expression from one representative clone of indicated ESC genotypes in the undifferentiated state (ESC) and at day 5 of RA differentiation (d5 RA). Error bars indicate SD from triplicate RT-PCR measurements in one experiment.

(F) As in (E), except that *Nanog* transcript levels were analyzed.

(G) Quantification of allele-specific *Xist* RNA cloud patterns from the experiment shown in (C) at days 6 and 10 of EB differentiation, given as mean of values from counts of two independent ESC clones of the indicated genotype. *Xist* expression from the 129 chromosome (targeted chromosome) is detected by both the *Xist* and *MS2* probes, whereas *Xist* expression from the CAST chromosome is only detected by the *Xist* probe. The graph depicts the percentage of cells where the intron 1-targeted 129 chromosome is coated by *Xist* RNA, as identified by colocalization of the *Xist* and *MS2* signals. * $p < 0.05$ by Student's t test with 500 *Xist* clouds analyzed for each sample.

See also Figures S3 and S4.

cells compared to 0.2%–0.8% in differentiating XY:2lox intron/*Tsix*-Stop cells (Figures 3E and 3G). We did not, however, see any significant intron 1-dependent effect on *Xist* RNA levels by RT-PCR comparing XY:2lox intron/*Tsix*-Stop and XY:1lox intron/*Tsix*-Stop cells (Figure 3D) or an increase in the number of H3K27me3 Xi-like accumulations (Figures 3F and 3H). Thus, even though *Xist* RNA was induced in a slightly larger proportion of differentiating cells in the absence of both *Tsix* and intron 1 than in the absence of either *Tsix* or intron 1, this upregulation does not appear to be sufficient to mediate H3K27me3 enrich-

ment on the targeted X chromosome, suggesting that the RNA does not efficiently coat the chromosome in these cells or that the recruitment of Polycomb proteins is affected. We conclude that these experiments reveal a subtle role of intron 1 in the control in *Xist* expression, which may be related to the weak skewing phenotype of XCI described above for differentiating intron 1 mutant heterozygous female ESCs (Figures 2 and S4).

In a second assay, we tested the consequence of intron 1 deletion upon modulation of global *Oct4* transcript levels. We first confirmed the previously reported relationship between

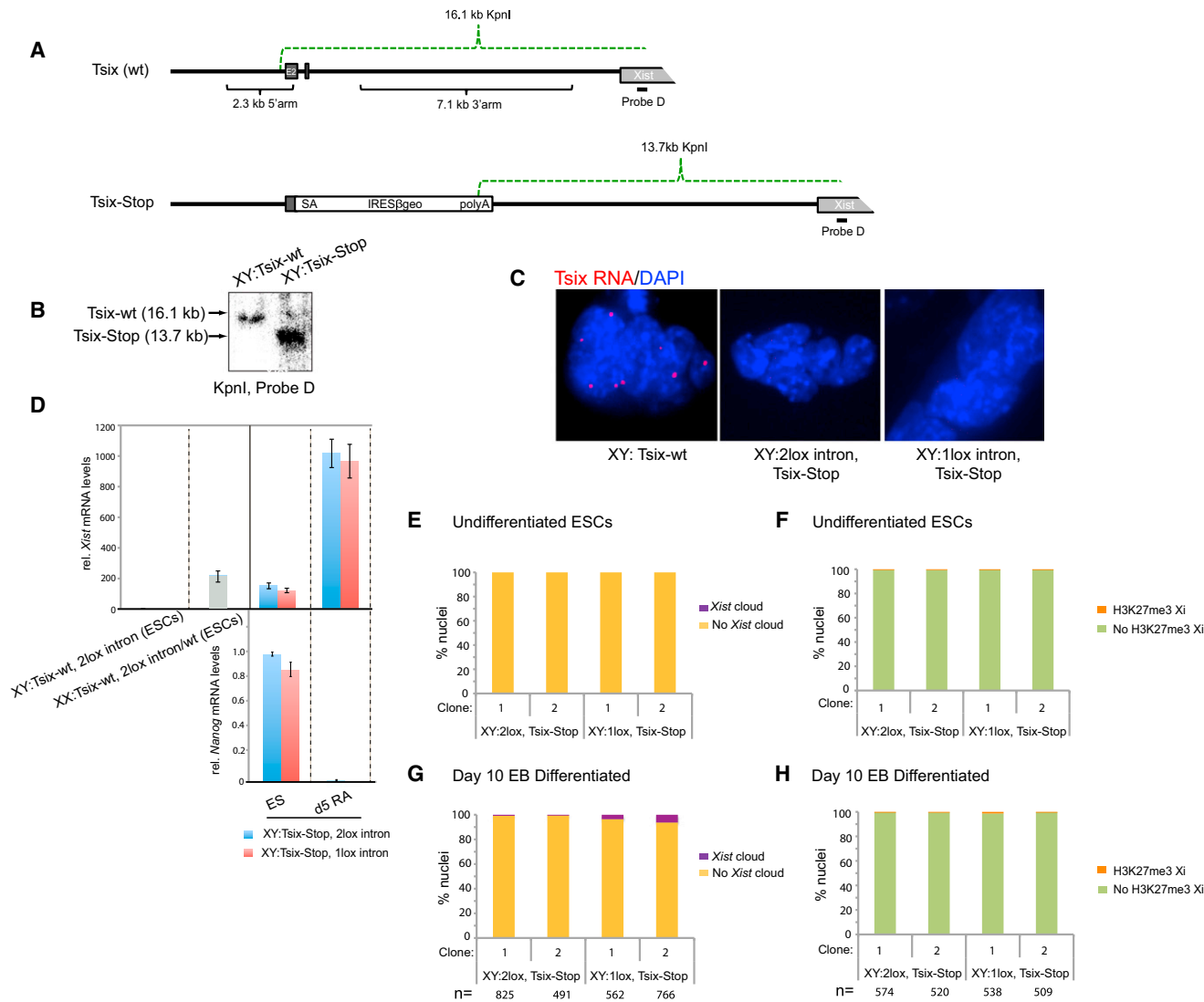


Figure 3. *Xist* RNA Pattern in Male ESCs Lacking *Tsix* and Intron 1

(A) Gene targeting and Southern blotting strategy schematic for the generation of the *Tsix*-Stop allele in male ESCs according to Sado et al. (2001) using the pAA2Δ1.7-targeting vector.

(B) Male 2lox and 1lox intron 1/*Tsix*-Stop male ESC clones were targeted with the *Tsix*-Stop allele. A correctly targeted 2lox intron 1/*Tsix*-Stop male ESC clone is shown in this Southern blot analysis.

(C) Strand-specific FISH for *Tsix* RNA (red) in undifferentiated male ESCs of the indicated genotypes, using an RNA probe, indicates the absence of the *Tsix* FISH signal in *Tsix*-Stop-targeted clones.

(D) Graph summarizing the transcript levels for *Nanog* and *Xist* normalized to *Gapdh* transcript levels as determined by RT-PCR from a representative clone of each genotype in the undifferentiated state (ES) and at day 5 of RA differentiation. Control *Xist* RNA levels from WT undifferentiated male and female ESCs are shown on the left. Error bars indicate SD from triplicate RT-PCR measurements in one experiment.

(E) Graph summarizing the percentage of undifferentiated ESCs of the given genotype with and without a *Xist* RNA cloud-like pattern. Two independent male ESC clones for each genotype were analyzed by *Xist* RNA FISH with an RNA probe, and 500 nuclei were assessed.

(F) As in (E), except that the percentage of undifferentiated ESCs with and without a H3K27me3 Xi-like accumulation is given.

(G) *Xist* RNA cloud quantification as in (E), except that *Nanog*-negative cells were quantified upon day 10 of EB differentiation.

(H) As in (F) for H3K27me3 patterns at day 10 of EB differentiation in indicated ESC lines.

See also Figure S5.

the decrease of *Oct4* levels and *Xist* RNA induction (Navarro et al., 2008; Donohoe et al., 2009). Specifically, upon *Oct4* depletion in the male ZHBTc4 ESC line, in which *Oct4* expression can be silenced acutely by the addition of doxycycline (Niwa et al.,

2000), *Xist* RNA levels were induced almost 100-fold 96 hr post-induction of *Oct4* repression (Figure S5A), and *Xist* RNA could be detected by FISH in a small number of cells (Figures S5B and S5C). Notably, we observed that *Oct4* transcript levels drop

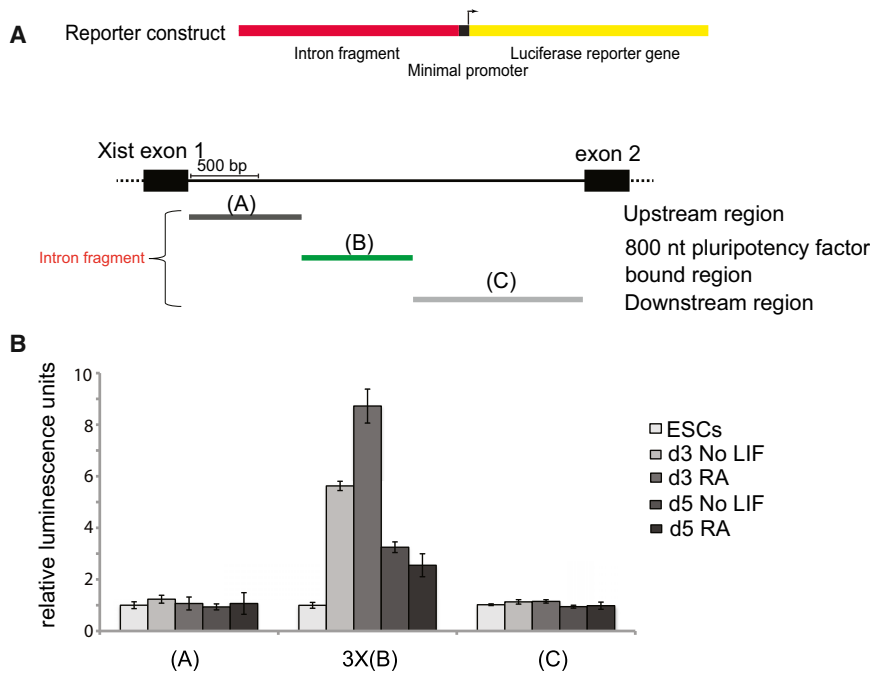


Figure 4. Enhancer Assay of *Xist* Intron 1

(A) Schematic representation of genomic fragments of the entire genomic intron 1 region cloned upstream of a luciferase reporter gene driven by a minimal promoter. The intronic region was broken up in three parts, with (B) representing the part bound by pluripotency factors and flanked by loxP sites as described in Figure 1 (Minkovsky/Plath allele), and (A) and (C) representing regions not bound by the pluripotency factors in ChIP-seq experiments (Figure S1). Note that (B) was concatenated 3× in the reporter construct.

(B) Three independent stable cell lines were generated by electroporation of male ESCs with the three constructs described in (A). Cells carrying the reporter constructs were selected with hygromycin, and an equal number of cells was plated and maintained in the undifferentiated state or differentiated for days 3 and 5 by LIF withdrawal and/or RA addition as indicated. After treatment, one-tenth of the cells in the well was analyzed by luciferase assay. For each reporter construct, values represent mean luminescence units normalized to values from the respective cell line in the undifferentiated state ($n = 3, \pm 1$ SD). See also Figure S6.

with faster kinetics than *Xist* RNA levels increase, suggesting that the effect of *Oct4* on intron 1 is indirect and may require efficient differentiation, which occurs at 96 hr post-*Oct4* repression, as indicated by the loss of the pluripotency factor Nanog (Figure S5D). In agreement with this conclusion, siRNA-mediated knockdown of *Oct4* in ESCs did not increase *Xist* RNA levels more than 2-fold after 72 hr, confirming a previous report by Donohoe et al. (2009) (Figure S5E). Furthermore, the absence of intron 1 did not significantly alter *Xist* RNA levels in female ESCs or in male ESCs lacking *Tsix* in *Oct4* knockdown conditions (Figure S5E). These data indicate that the slight increase in *Xist* levels immediately upon *Oct4* depletion is independent of intron 1.

Intron 1 Acts as an Enhancer in a Reporter Assay in Differentiating ESCs

The model of pluripotency factor binding to intron 1 to repress *Xist* motivated us to directly assess whether intron 1 behaved as a silencer in ESCs in a reporter assay. We transfected constructs with intron 1 or control sequences upstream of a minimal promoter driving luciferase and did not see intron 1-dependent decreases in reporter activity (data not shown). The small effect of intron 1 deletion on *Xist* RNA levels detected in differentiating ESCs in the absence of *Tsix* motivated us to revisit these experiments and instead investigate whether *Xist* intron 1 represents a developmentally regulated enhancer that becomes active upon induction of differentiation. We therefore tested transactivation activity of intron 1 in undifferentiated and differentiating ESCs using stably integrated luciferase reporter constructs (Figure 4). Male ESCs were electroporated with hygromycin resistance-bearing constructs containing either the part of intron 1 that we deleted in our experimental cell lines or two control sequences representing the upstream and downstream flanking regions of the intron 1 region (Figure 4A). The

experimental intron 1 region ((B) in Figure 4B) was cloned in triple copy to amplify any putative enhancer activity of this region. Pooled clones were subjected to monolayer differentiation by LIF withdrawal with and without retinoic acid (RA) treatment. Only cells bearing the intron 1 construct covering the pluripotency factor binding site showed a robust increase in luciferase activity upon differentiation (Figure 4B). In agreement with the notion that intron 1 does not act as an active enhancer in undifferentiated ESCs, we did not find a histone acetylation mark characteristic of active enhancers, namely H3K27ac, examining our own and published ChIP-seq data sets from ESCs, despite binding of intron 1 by a battery of pluripotency factors and p300 in undifferentiated ESCs (mouse ENCODE; Creyghton et al., 2010; data not shown).

We also considered recently published spatial organization data that demonstrated that the *Xist* gene lies in a topologically associating domain (TAD) with genes encoding the noncoding RNAs *Ftx* and *Jpx/Enox* and the protein-coding genes *Rnf12/Rlim*, *Zcchc13*, and *Slc16a2* (Nora et al., 2012). It has been proposed that promoters and enhancers predominantly interact (loop) within TADs (Dixon et al., 2012; Nora et al., 2012). Notably, significant intra-TAD contacts originating from within intron 1 of *Xist*, indicative of putative enhancer/promoter looping, were only found in differentiated and not in undifferentiated ESCs (Nora et al., 2012) (Figure S6A), consistent with our finding of reporter activity upon differentiation. However, similar to our result that *Xist* levels in female and male ESCs did not significantly change in the absence of intron 1, we also did not see intron 1-dependent transcriptional differences in the three genes that come in contact with intron 1 within the *Xist*-containing TAD, before and during differentiation (Figure S6B). Thus, even though intron 1 is pluripotency factor bound in ESCs, it may only gain significant enhancer activity upon differentiation

though still not to an extent where deletion affects transcription of *Xist* or of neighboring protein-coding genes.

Together, these ex vivo studies in undifferentiated and differentiating male and female ESCs point to a minor role for intron 1 in the regulation of *Xist* expression, uncovered only when another *Xist* repressor is deleted, and some aspect of X chromosome choice (potentially also through slight modulation of *Xist* RNA levels). These data do not support intron 1 as a main aspect of the mechanism of transcriptional repression of *Xist*, at least in this tissue culture model.

Mice Are Normal in the Absence of Intron 1

Next, we assayed the significance of intron 1 in vivo. Our male ESCs deleted for intron 1 (1lox) were injected into C57BL/6 blastocysts. Chimeras were obtained at high efficiency and bred with C57BL/6 females to obtain germline transmission of the mutant allele. Subsequently, the 1lox intron 1 allele showed normal propagation through the maternal or paternal germline, and mice completely lacking intron 1 (crossing 1lox/1lox females with 1lox males) could be efficiently bred without any female-specific defect (Figure 5A). Because X chromosome reactivation occurs in the female germline and is likely essential for female fertility, we assessed litter size of the F2 generation of female homozygous knockout mice, and we found their litter sizes unaffected (data not shown), indicating that intron 1 is not essential in mice.

To strengthen these observations of normal transmission of the intron 1 mutation and rule out that genetic background obscured a potential intron 1 phenotype in vivo, we generated a second mouse model carrying an independent intron 1 mutation. We generated mice using previously published 129/CAST F1 female ESCs in which a larger (1.815 kb) region harboring most of intron 1 was deleted on the 129 X chromosome (Barakat/Gribnau allele) (Figure S1A; Barakat et al., 2011). Using these ESCs, we previously observed a slight upregulation of *Xist* RNA levels on the deleted chromosome upon induction of differentiation (Barakat et al., 2011), in agreement with results obtained using the Minkovsky/Plath allele, indicating skewing of X inactivation toward the intron 1-deleted chromosome. Importantly, this second mouse model also displayed normal Mendelian transmission of the intron 1 lox allele (Figure 5B).

To assay whether random XCI has occurred in female mice carrying a Xp lacking intron 1 and a maternally inherited WT X chromosome, and whether the lack of the intron leads to any skewing of XCI in vivo, we analyzed the allele-specific expression of *Xist* and two X-linked genes, *Mecp2* and *G6pdx*, in polymorphic heterozygous females (1lox^{C57BL/6}/WT^{CAST/Ei}) and a WT control (WT^{C57BL/6}/WT^{CAST/Ei}). In these mice, the C57BL/6 X chromosome was transmitted from the father and the CAST/Ei WT X from the mother. Allele-specific expression analysis was performed using semiquantitative RT-PCR on RNA isolated from various tissues (Figures 5C–5E). In these experiments, we used the Barakat/Gribnau mouse model described in Figures 5B and S1A. Normally, the paternal X chromosome initially undergoes imprinted XCI, which is reversed in the epiblast cells of the preimplantation blastocyst to allow subsequent random XCI. The intron 1 region has been implicated to be important for Xi reactivation in the ICM, and thus, if the absence of intron

1 prevents reactivation of imprinted XCI, we may observe nonrandom XCI in the adult mouse (Navarro et al., 2008).

However, we did not find differences in allele-specific expression pattern in the presence and absence of intron 1 in heterozygous female mice (Figures 5C–5E). As expected, the C57BL/6 *Xist* allele is more often expressed than the CAST/Ei X, consistent with a modifier effect, likely resulting in more cells with an inactivated C57BL/6 X (Cattanach and Isaacson, 1967). Because of the stochastic and clonal nature of XCI patterns in the adult mouse, variations in skewing toward *Xist* RNA from the C57BL/6 allele ranged from 50% to 90% (Figures 5C and 5E). Notably, we did not see a preference of *Xist* upregulation on the intron 1-deleted X chromosome in tissues of the adult mouse in vivo, albeit we observed slightly skewed *Xist* RNA levels in heterozygous-differentiating female ESCs carrying the same mutant intron 1 allele in vitro (Barakat et al., 2011). In agreement with this notion, the X-linked genes *Mecp2* and *G6pdx*, both subject to silencing on the Xi, showed reciprocal and intron 1-independent levels of expression from the C57BL/6 chromosome compared to *Xist*, as would be expected from the fact that the *Xist*-expressing chromosome is more likely to be silent (Figures 5D and 5E). These data suggest that the paternal transmission of the intron 1 mutation does not interfere with reactivation of imprinted XCI and subsequent random XCI. A reverse cross in which the maternal allele lacked intron 1 also resulted in random XCI (data not shown). In summary, the intron 1 genomic region is dispensable in the mouse and does not critically control *Xist* expression and skewing of XCI in vivo.

Intron 1 Is Not Required for Loss of *Xist* RNA upon Reprogramming to iPSCs

Although there was no dramatic effect on XCI state in vivo, we sought to understand the requirement for intron 1 in *Xist* silencing associated with reprogramming to iPSCs. We have shown previously that female iPSCs derived from mouse embryonic fibroblasts (MEFs) carry two active X chromosomes, where *Xist* is efficiently repressed and *Tsix* upregulated, as seen in mouse ESCs (Maherali et al., 2007). Another study suggested that Xi reactivation occurs late in reprogramming at around the time pluripotency genes become expressed, again suggesting that pluripotency transcription factors could contribute to Xi reactivation and the silencing of *Xist*, potentially via binding to intron 1 (Stadtfield et al., 2008). To test the role of intron 1 in the *Xist*-silencing process during reprogramming, we bred male mice carrying the 2lox intron 1 allele (obtained upon blastocyst injection of our male 2lox ESCs described in Figure 1, Minkovsky/Plath allele) with female mice heterozygous for a *Xist* knockout allele (Marahrens et al., 1997), yielding female XX:2lox intron/ Δ *Xist* MEFs. Due to the presence of the *Xist* knockout allele, the X chromosome bearing the conditional intron 1 allele is exclusively inactivated in vivo by normal developmental mechanisms (Marahrens et al., 1998). MEFs isolated from E14.5 embryos had uniform *Xist* coating (Figure 6C) and were transduced with retroviruses encoding the reprogramming factors Oct4, Sox2, and Klf4, and subsequently infected with adenovirus encoding Cre recombinase at day 4 of reprogramming to efficiently delete the intron 1 region or with titer-matched empty adenovirus in control samples (Figure 6A). This

A Minkovsky/Plath Allele

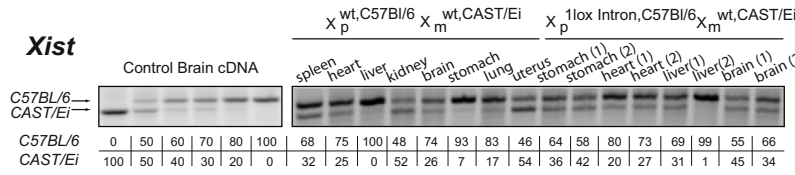
Paternal Genotype	Maternal Genotype	Average Litter Size	Offspring				p-Value
			♂		♀		
XY:+	XX:1lox/+	7.2	XY:+	XY:1lox	XX:+/+	XX:1lox/+	>0.25 ^a
			10	10	6	10	
XY:1lox	XX:1lox/+	6.7	XY:+	XY:1lox	XX:1lox/+	XX:1lox/1lox	>0.25 ^a
			10	12	14	11	
XY:1lox	XX:1lox/1lox	8.0	XY:1lox		XX:1lox/1lox		>0.25 ^b
				23		17	

B Barakat/Gribnau Allele

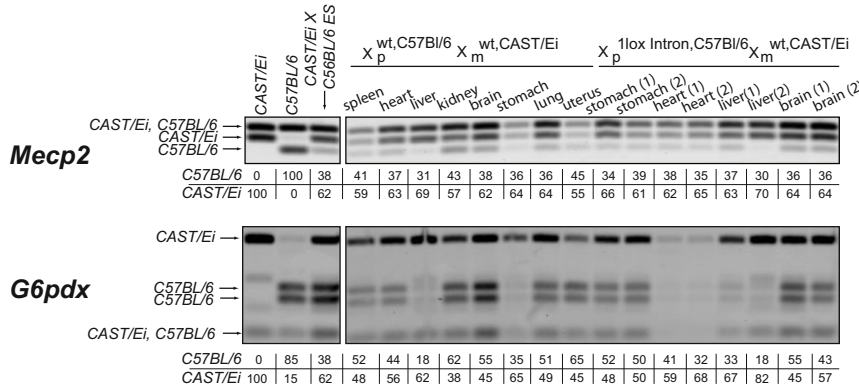
Paternal Genotype	Maternal Genotype	Average Litter Size	Offspring				p-Value
			♂		♀		
XY:+	XX:1lox/+	6.7	XY:+	XY:1lox	XX:1lox/1lox	XX:1lox/+	>0.10 ^a
			2	6	3	9	
XY:1lox	XX:+/+	6.5	XY:+		XX:1lox/+		>0.25 ^b
				11		15	
XY:1lox	XX:1lox/+	6.1	XY:+	XY:1lox	XX:1lox/+	XX:1lox/1lox	>0.25 ^a
			13	15	8	13	
XY:1lox	XX:1lox/1lox	5.3	XY:1lox		XX:1lox/1lox		>0.25 ^b
				32		37	

^{a,b} Chi-square test for expected 1:1:1:1 (a) or 1:1 (b) ratio

C *Xist*



D



E

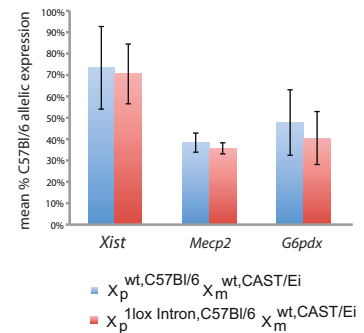


Figure 5. Transmission of the Intron 1 Mutation In Vivo

(A) Table summarizing the number and genotypes of offspring from indicated mouse crosses using the intron 1 allele generated in the Plath lab (see Figure 1, Minkovsky/Plath allele).

(B) As in (A), except that mice carrying a second, independent intron 1 deletion generated by the Gribnau lab were crossed (see Figure S1 for comparison of alleles; Barakat et al., 2011).

(C) Allele-specific RT-PCR analysis of *Xist* RNA detecting a length polymorphism that distinguishes *Xist* RNA originating from the C57BL/6 and CAST X chromosome in organs of one female WT mouse and two littermate heterozygous 1lox/WT mice obtained by crossing a C57BL/6 male (with and without the intron 1 1lox allele) with a WT CAST/Ei female. Panel includes controls on the left mixing pure C57BL/6 and CAST/Ei brain cDNA template in given ratios. Numbers below the tissue samples represent the relative band intensity for the C57BL/6 and CAST/Ei *Xist* allele determined by comparison with the control samples.

(D) Examination of tissues as in (C) for allelic expression of X-linked genes *MeCP2* (top) and *G6pdx* (bottom) by RFLP RT-PCR. Panel includes controls (left) from pure C57BL/6 or CAST/Ei mice as well as RNA isolated from a polymorphic C57BL/6 and CAST/Ei ESC line.

(E) Graph averaging the allele-specific expression data in (C) and (D) across all tissue and mice per genotype \pm 1 SD.

experimental setup allowed us to test the role of intron 1 in reprogramming efficiency for the same infected fibroblast population. Genotyping confirmed that Ad-Cre addition resulted in efficient deletion of the intron 1 region (Figure 6B). To test whether intron 1 deletion affects the efficiency of reprogramming, we determined the number of Nanog-expressing colonies at day 13 after reprogramming factor introduction because

Nanog expression has been shown to mark faithfully reprogrammed cells in retroviral reprogramming experiments (Maherali et al., 2007). We found a comparable number of Nanog+ colonies in the presence and absence of intron 1 (Figure 6D). Normally, at this point of reprogramming, *Xist* RNA coating is just lost in Nanog+ cells (K.P. and J. Tchiew, unpublished data). In agreement with this notion, an examination of all Nanog+ cells for

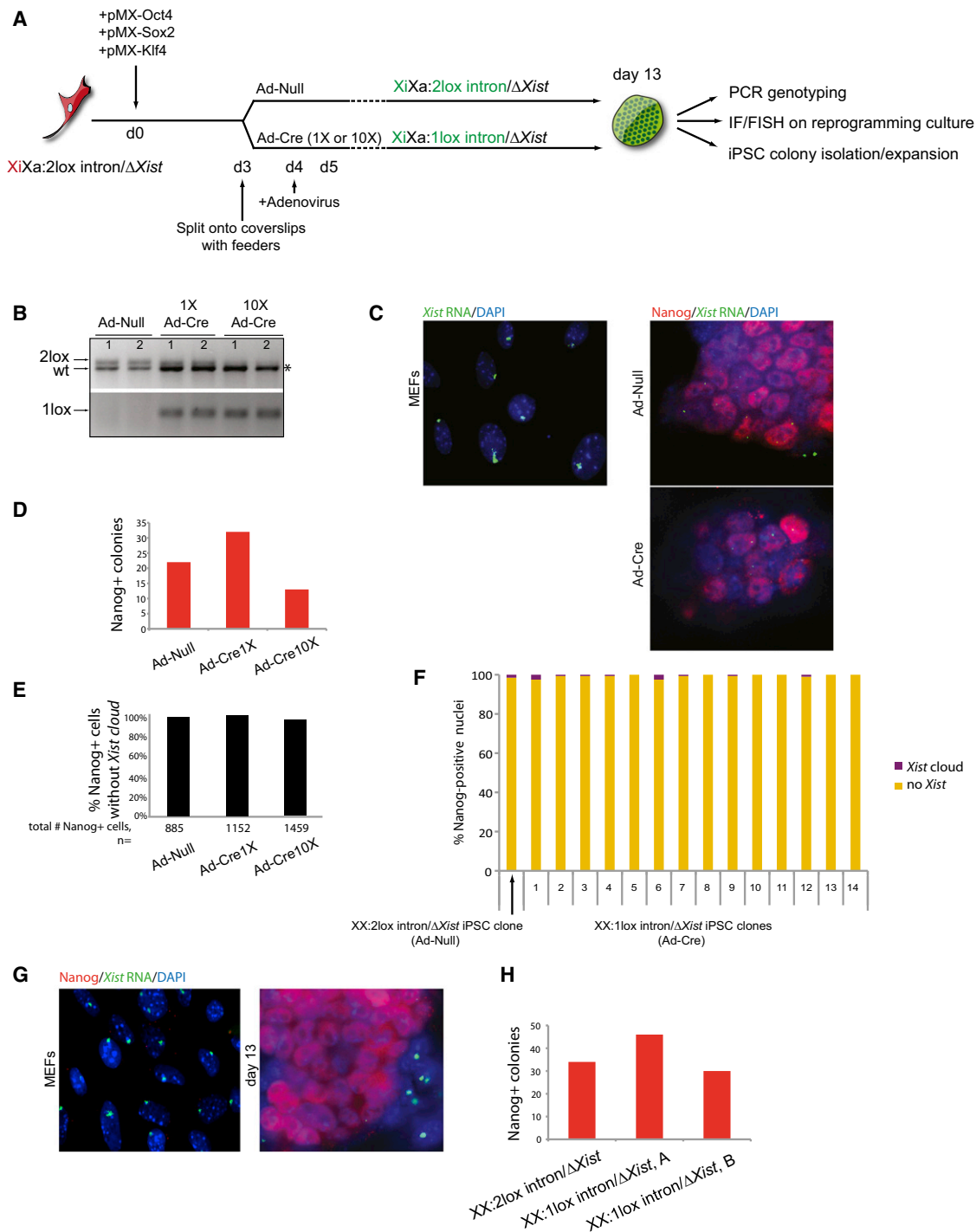


Figure 6. The Absence of Intron 1 on the Xi Does Not Interfere with Loss of *Xist* RNA Coating upon Reprogramming of MEFs to iPSCs

(A) Schematic representation of the reprogramming experiment with female MEFs bearing the conditional intron 1 allele on the Xi and a *Xist* knockout allele on the Xa. Reprogramming was induced by infection with pMX retroviruses encoding the reprogramming factors, and the reprogramming culture was split at day 3 postinfection. Deletion of the conditional intron 1 allele was induced by delivery of 1x or 10x adenoviral particles carrying Cre recombinase, performed at day 4. Control 1x Ad Null treatment was done in parallel. At day 13 of reprogramming, efficient deletion of intron 1 was assessed by genotyping, reprogramming efficiency was determined by Nanog+ colony count, and loss of *Xist* RNA coating in Nanog+ cells was examined by IF/FISH. In addition, individual colonies were picked, expanded, and analyzed further.

(B) PCR genotyping for the presence of the 2lox and 1lox intron 1 alleles in reprogramming cultures at day 13, using primers pairs A and C (top panel) or B and C (bottom panel) (as in Figure 1F), indicates efficient deletion of intron 1 upon Ad-Cre treatment. "1" and "2" represent independent reprogramming samples. The asterisk marks the WT allele, which is attributed to the presence of feeder cells in reprogramming cultures.

(legend continued on next page)

the presence or absence of a *Xist* RNA cloud demonstrated that nearly all Nanog⁺ cells carrying the 2lox intron 1 allele (Ad Null-reprogramming cultures) lack a *Xist* RNA cloud at day 13 of reprogramming (Figures 6C and 6E). Importantly, even in the absence of intron 1 (Ad-Cre samples), Nanog⁺ cells displayed loss of the *Xist* RNA cloud (Figures 6C and 6E) and of the Xi-like H3K27me₃ focus (data not shown). Furthermore, from the Ad-Cre-treated reprogramming cultures, 14 iPSC clones were isolated and clonally propagated and all confirmed to have lost both intron 1 and the *Xist* RNA cloud, demonstrating the efficient deletion of the intronic sequence early in reprogramming (Figure 6F). To ensure that the ability of an intron 1-deleted Xi chromosome to downregulate *Xist* was not due to intron 1-dependent events occurring within the first 4 days of reprogramming, i.e., prior to Cre-mediated deletion, we also reprogrammed MEFs carrying a germline-transmitted 1lox intron allele. These XX:1lox intron/ Δ *Xist* MEFs displayed normal *Xist* RNA coating before reprogramming (detectable in 95% of the cells) and lost *Xist* RNA in Nanog⁺ colonies (Figure 6G). When comparing to XX:2lox intron/ Δ *Xist* MEFs, MEFs lacking intron 1 form Nanog⁺ colonies with similar efficiencies (Figure 6H). Together, these studies rule out that *Xist* intron 1 is necessary for the downregulation of *Xist* in reprogramming to pluripotency.

DISCUSSION

In summary, our data argue that *Xist* intron 1 does not represent an essential tether-coupling repression of both *Xist* and XCI to the pluripotent state. ESCs lacking intron 1 do not dysregulate *Xist* expression in the undifferentiated state nor upon in vitro differentiation, reprogramming to the iPSC state leads to *Xist* repression on a Xi lacking intron 1, and mice lacking intron 1 do not display any of the gross reproductive abnormalities that would be expected if XCI was perturbed.

The deletion of intron 1 represents a clean experimental system to probe the functional role of a genomic element that displays very strong pluripotency transcription factor binding, unhampered by the secondary effects on initiation of XCI associated with global modulation of protein factors implicated in the maintenance of the pluripotent state. Although correlative binding studies were supported in part by *Xist* dysregulation in ESC lines with inducible deletions of the pluripotency factors Nanog and Oct4, our study cautions against extrapolating these findings to the behavior of WT ESCs and mice. In the

case of the ZHBTc4 Oct4-repressable cell line, a compromised pluripotency network may result in Rnf12 upregulation followed by downregulation of the pluripotency factor Rex1, sufficient to trigger XCI in male cells independent of intron 1 (Barakat et al., 2011; Gontan et al., 2012). We also noted that ZHBTc4 ESCs lack pinpoint *Tsix* signal and draw a corollary between their *Xist* upregulation and our male ESCs deleted for *Tsix* (that, when differentiating, have a significantly greater number of *Xist* clouds upon deletion of intron 1).

In light of the two mild phenotypes (skewing effect of deleting intron 1 in female ESCs heterozygous for the allele and the slight increase in *Xist* clouds in *Tsix* and intron 1-deleted differentiating male ESCs), we hypothesize that intron 1 loss leads to mild destabilization of *Xist* transcriptional repression at the transition to the differentiated state, in the narrow development window of XCI initiation. Unable to capture a transcriptional difference in *Xist* levels at the onset of in vitro differentiation, we believe that more sensitive methods of transcript quantitation or investigation of chromatin state may address this hypothesis.

We noted a discrepancy between the ex vivo XCI-skewing phenotype and the normally occurring in vivo XCI choice in the absence of the intron. The lack of an intron 1 deletion effect in adult mice and in ESC differentiation induced by bFGF/Activin (Figure S5), which is sensitive to clonogenic skewing of XCI because of serial passage and outgrowth of few cells (unlike monolayer differentiation; Chenoweth and Tesar, 2010), suggests that *Xist* regulation is more robust in vivo than in vitro in the absence of the intron 1. For instance, slightly different *cis*-acting elements could be used in vivo and in vitro for regulating *Xist* expression. Thus, the cell culture-observed favoring of the intron-deleted *Xist* could not be organismally relevant, or the stochastic developmental nature of XCI could overshadow the effect.

It seems that the regulation of *Xist*, at the helm of a chromosome-wide program of gene expression, is genetically ensured by a complex multifactor mechanism. The dispensability of intron 1 for repression of *Xist* may be mouse specific because mice appear to be unique in the functionality of *Tsix* and also in the sufficiency of *Xist* activators such as Rnf12 to elicit *Xist* upregulation: addition of one copy of Rnf12 is sufficient to drive *Xist* expression in undifferentiated female ESCs (Jonkers et al., 2009). Other eutherians such as bovines and humans, with truncated and likely nonfunctional *TSIX*, may rely more on intron 1-dependent mechanisms for *Xist* repression (Chureau et al., 2002). Therefore, evolution of the overlapping *Tsix* gene and

(C) FISH of starting MEFs before introduction of pMX retrovirus displaying *Xist* RNA coating (left) and immunostaining/FISH images (right) of representative Nanog⁺ colonies in reprogramming cultures treated with Ad Null and Ad-Cre, respectively, at day 13 of reprogramming, showing Nanog expression (red), FISH for *Xist* RNA using a DNA probe (green), and DAPI (blue). Note that Nanog⁺ cells at this stage of reprogramming display a biallelic pinpoint signal when using the double-stranded DNA probe, which can be attributed to *Tsix* expression.

(D) Graph summarizing reprogramming efficiency by counting Nanog⁺ colonies at day 13.

(E) Graph showing the percentage of Nanog⁺ cells without a *Xist* RNA cloud at day 13 of reprogramming. All Nanog⁺ cells (number is given) on the reprogramming culture coverslip were counted and analyzed for the *Xist* signal.

(F) The graph summarizes the percentage of Nanog⁺ nuclei with and without *Xist* RNA clouds in individually expanded iPSC clones from Ad Null or Ad-Cre reprogramming cultures (200 nuclei counted for each iPSC line). Genotyping of all iPSC clones confirmed that intron 1 was deleted in all iPSCs expanded from Ad-Cre reprogramming cultures.

(G) MEFs were obtained from XX:1lox intron/ Δ *Xist* embryos and reprogrammed with Oct4, Sox2, and Klf4. Immunostaining/FISH images show the presence of normal *Xist* RNA coating in the starting MEFs and the absence of *Xist* RNA coating in resulting Nanog⁺ colonies at day 13 of reprogramming.

(H) Graph showing counts of Nanog⁺ colonies at day 13 of reprogramming for two different XX:1lox intron/ Δ *Xist* MEF preparations (A and B, from different matings) and one XX:2lox intron/ Δ *Xist* line that was reprogrammed in parallel.

the network of XCI activators in mice may have become the dominant mechanism in *Xist* repression.

EXPERIMENTAL PROCEDURES

Generation of Mutant mESCs and Mice

Xist intron 1 transgenic mice analyzed in Figures 5B–5E were generated from polymorphic $X^{Xist:2loxneo\ intron\ (129/Sv)} X^{Xist: WT\ (CAST/Ei)}$ ESC line 29, in which a 1.8 kb region of *Xist* intron 1 was replaced by a floxed neomycin cassette (Barakat et al., 2011). Germline transmission was verified by genotyping for the presence of the neomycin cassette integrated in the intron 1 region of *Xist*, and XX:2lox-neo/WT females were bred to males expressing pCAGGS-Cre, to loop out the selection cassette. Loopout of the selection cassette was verified by PCR on genomic tail tip-derived DNA. All other intron 1-mutant ESC lines and mice carrying the Plath/Minkovsky allele were derived from a targeting construct generated by cloning the respective genomic fragments representing the 5' and 3' homology regions into the pCR11 plasmid vector upon PCR amplification (see Table S1 for list of primers used). The 800 bp of intron sequence with a 5' loxP site was ligated between a 2.2 kb 5' homology arm and 3' 2.6 kb homology arm by AgeI/NotI subcloning. A positive-negative CMV-HygroTK selection cassette flanked by loxP sites was inserted into the unique NotI site. A diphtheria toxin gene (PGK-DTA) was inserted into a unique backbone EcoRI site. A total of 40 μ g of plasmid was linearized by MluI digestion and electroporated into male ESCs (V6.5 line; F1 between C57BL/6 and 129SV/Jae) and into female F1 2-1 ESCs carrying the MS2 tag in the final large exon of *Xist* (F1 between C57BL/6 and CAST/Ei) cells cocultured with drug-resistant DR4 MEFs (Jonkers et al., 2008; Tucker et al., 1997). Hygromycin selection (140 μ g/ml) was started 1 day after, and clones were screened by Spel/KpnI digest and both 5' and 3' external probes. BmtI digest and 3' external probe were used to assess allelism of targeting in F1 2-1 clones. Targeting efficiency was 30% in V6.5 and 1% in F1 2-1 cells. Two independent V6.5 and one F1 2-1 clones were expanded, electroporated with pPAC-Cre plasmid, and selected with G418 (300 μ g/ml) for 8 days. Southern blot screening was performed with a 5' probe and XbaI digest for 1lox and Spel/KpnI for 2lox clones. All subsequent intron 1 genotyping was performed by PCR. For intron 1/*Tsix*-Stop double-transgenic ESC clones, XY:2lox and XY:1lox V6.5 clones were targeted with pAA2 Δ 1.7 and screened by Southern blot as previously described by Sado et al. (2001). XY:1lox and XY:2lox V6.5 ESCs were microinjected into C57BL/6 blastocysts to produce chimeric mice following standard procedures. High-agouti coat color-contributing chimeras were bred with C57BL/6 females for germline transmission. All animal experiments were in accordance with the legislation of the Erasmus MC Animal Experimental Commission and the UCLA Animal Research Committee.

Cell Culture, Differentiation, and Reprogramming Methods

ESCs were grown on irradiated DR4 MEFs in standard media (DMEM supplemented with 15% FBS, nonessential amino acids, L-glutamine, penicillin-streptomycin, β -mercaptoethanol, and 1,000 U/ml LIF). Prior to induction of RA differentiation, cells were feeder depleted for 45 min on gelatinized plates and plated at a density of 5.0×10^4 cells/6-well in MEF media (same as ESC media except 10% FBS and excluding LIF). One day later, MEF medium was supplemented with 1 μ M all *trans* RA (Sigma-Aldrich) or with DMSO only (LIF withdrawal) and refreshed every 2 days. For EB differentiation, ESCs were preplated on gelatin overnight to feeder deplete, briefly trypsinized, and put in MEF media for suspension culture on bacterial culture plates for 4 days, then plated on gelatinized coverslips for another 2 or 6 days. For FGF/Activin differentiation, ESCs were feeder depleted and 2.0×10^4 cells plated on six wells pretreated with fibronectin in DMEMF12/B-27/N-2 (Invitrogen) supplemented with FGF-2 (R&D Systems; 40 ng/ml) and Activin A (Pepro-Tech; 20 ng/ml). Medium was changed daily, and colonies were manually passaged onto fibronectin several times then at passage 4 returned to feeder cells. ZHBTc4 ESCs were induced to differentiate with 1 μ g/ml doxycycline (resulting in acute repression of Oct4) in standard ESC media (Niwa et al., 2000). For reprogramming, primary MEFs were derived at E14.5, and three-factor retroviral reprogramming was performed following previously published methods by Maherali et al. (2007).

ChIP

ChIP was performed according to previously published methods by Maherali et al. (2007). In summary, formaldehyde-crosslinked chromatin fragments were generated by sonication, and 150 μ g of material was precleared with Protein A Sepharose beads. IP was performed overnight with 5 μ g antibodies targeting Oct4 (R&D Systems; AF1759) or Sox2 (R&D Systems; AF2018), or with normal goat IgG (Santa Cruz Biotechnology; sc-2028) and subsequent incubation with protein A Sepharose beads for 3 hr. Beads were washed and eluted in TE/0.67% SDS. Both IP and input samples were reverse cross-linked overnight at 65°C and treated with RNase A and Proteinase K before DNA phenol-chloroform purification. The proportion of input material immunoprecipitated was calculated using standard curves constructed from input serial dilutions and comparing fractional measurements in IP and input relative to a known region positive for Oct4 and Sox2 binding (Rest; van den Berg et al., 2008). ChIP with goat IgG antibody did not find any enrichment (data not shown).

Immunofluorescence and FISH Analysis

Cells were plated on glass coverslips (and in the case of EB differentiation, permeabilized with 5 min washes of ice-cold CSK buffer, followed by CSK buffer with 0.5% Triton X-100, and another wash in CSK buffer, washed once with PBS, and fixed for 10 min in 4% paraformaldehyde) (Plath et al., 2003). Immunostaining with antibodies against Nanog (BD Pharmingen; 560259) and H3K27me3 (Active Motif 39155) and combined immunostaining/FISH with double-strand *Xist* DNA probe labeled with FITC were performed as previously reported and mounted with Prolong Gold reagent with DAPI (Tchiew et al., 2010). *Xist* and *Tsix* strand-specific RNA probes were made by in vitro transcription of T3-ligated PCR products of cDNA templates using Riboprobe system T3 (Promega) with Cy3-CTP (VWR) or FITC-UTP (PerkinElmer) (Maherali et al., 2007).

qRT-PCR Analysis and Allele-Specific qRT-PCR

Cells were harvested from a 6-well format in TRIzol (Invitrogen), and RNA purification was performed with the RNeasy kit (QIAGEN) according to manufacturer's instructions with on-column DNase treatment (QIAGEN). cDNA was prepared using SuperScript III (Invitrogen) with random hexamers, and qRT-PCR was performed using a Stratagene Mx3000 thermocycler with primers listed in Table S1. Results were normalized to Gapdh by the Δ Ct method. To assess XCI skewing in adult mice, parts of organs were collected, snap frozen, and triturated using micropestles in 1 ml of TRIzol reagent. After an additional centrifugation to clear debris, 700 μ l was added to 300 μ l fresh TRIzol, and RNA was purified following manufacturer's instructions. RNA was reverse transcribed with SuperScript II (Invitrogen) using random hexamers. Allele-specific *Xist* expression was analyzed by RT-PCR amplifying a length polymorphism using primers *Xist* LP 1445 and *Xist* LP 1446. To determine allele-specific X-linked gene expression of *Mecp2* and *G6pdx* primers, MeCP2-*Ddel*-F and R and G6PD-*ScrFI*-F and R were used to amplify respective restriction fragment-length polymorphisms (RFLPs). PCR products were gel purified and digested with the indicated restriction enzymes and analyzed on a 2% agarose gel stained with ethidium bromide. Allele-specific expression was determined by measuring relative band intensities using a Typhoon image scanner and ImageQuant software.

Luciferase Enhancer Assay

XY:2lox ESCs were transfected by electroporation with 40 μ g of one of three BamHI-linearized pgl4.27-cloned constructs carrying different intron fragments (Promega; Table S1) and transferred to hygromycin selection (140 μ g/ml) 1 day later. After serial passaging and outgrowth of stable transfectants, 1.0×10^5 or 2.0×10^4 ESCs were seeded for differentiation with and without (no LIF) RA for 3 and 5 days and harvested along with 2.0×10^5 ESCs and measured for luciferase activity with the luciferase assay system (Promega).

SUPPLEMENTAL INFORMATION

Supplemental Information includes six figures and one table and can be found with this article online at <http://dx.doi.org/10.1016/j.celrep.2013.02.018>.

LICENSING INFORMATION

This is an open-access article distributed under the terms of the Creative Commons Attribution-NonCommercial-No Derivative Works License, which permits non-commercial use, distribution, and reproduction in any medium, provided the original author and source are credited.

ACKNOWLEDGMENTS

K.P. is supported by the NIH (DP2OD001686 and P01 GM099134), CIRM (RN1-00564 and RB3-05080), and the Eli and Edythe Broad Center of Regenerative Medicine and Stem Cell Research at UCLA. A.M. is supported by National Research Service Award AG039179. K.P. and A.M. are supported by funds from the Iris Cantor-UCLA Women's Health Center Executive Advisory Board. J.G. was supported by NWO VICI and ERC starting grants. We thank Ying Wang of the UCLA Transgenic Core Facility for blastocyst injections; Takashi Sado for his pAA2Δ2.17 Tsix-targeting construct and helpful input; and Elyse Rankin-Gee, Dana Case, Matthew Denholtz, Rebecca Rojansky, Konstantinos Chronis, Ritchie Ho, Bernadett Papp, and Sanjeet Patel for advice and experimental support.

Received: November 30, 2012

Revised: February 12, 2013

Accepted: February 14, 2013

Published: March 21, 2013

REFERENCES

- Barakat, T.S., Gunhanlar, N., Pardo, C.G., Achame, E.M., Ghazvini, M., Boers, R., Kenter, A., Rentmeester, E., Grootegoed, J.A., and Gribnau, J. (2011). RNF12 activates *Xist* and is essential for X chromosome inactivation. *PLoS Genet.* 7, e1002001.
- Brockdorff, N., Ashworth, A., Kay, G.F., Cooper, P., Smith, S., McCabe, V.M., Norris, D.P., Penny, G.D., Patel, D., and Rastan, S. (1991). Conservation of position and exclusive expression of mouse *Xist* from the inactive X chromosome. *Nature* 351, 329–331.
- Brown, C.J., Ballabio, A., Rupert, J.L., Lafreniere, R.G., Grompe, M., Tonlorenzi, R., and Willard, H.F. (1991). A gene from the region of the human X inactivation centre is expressed exclusively from the inactive X chromosome. *Nature* 349, 38–44.
- Cattanach, B.M., and Isaacson, J.H. (1967). Controlling elements in the mouse X chromosome. *Genetics* 57, 331–346.
- Chaumeil, J., Le Baccon, P., Wutz, A., and Heard, E. (2006). A novel role for *Xist* RNA in the formation of a repressive nuclear compartment into which genes are recruited when silenced. *Genes Dev.* 20, 2223–2237.
- Chen, X., Xu, H., Yuan, P., Fang, F., Huss, M., Vega, V.B., Wong, E., Orlov, Y.L., Zhang, W., Jiang, J., et al. (2008). Integration of external signaling pathways with the core transcriptional network in embryonic stem cells. *Cell* 133, 1106–1117.
- Chenoweth, J.G., and Tesar, P.J. (2010). Isolation and maintenance of mouse epiblast stem cells. *Methods Mol. Biol.* 636, 25–44.
- Chow, J., and Heard, E. (2009). X inactivation and the complexities of silencing a sex chromosome. *Curr. Opin. Cell Biol.* 21, 359–366.
- Chureau, C., Prissette, M., Bourdet, A., Barbe, V., Cattolico, L., Jones, L., Eggen, A., Avner, P., and Duret, L. (2002). Comparative sequence analysis of the X-inactivation center region in mouse, human, and bovine. *Genome Res.* 12, 894–908.
- Chuva de Sousa Lopes, S.M., Hayashi, K., Shovlin, T.C., Mifsud, W., Surani, M.A., and McLaren, A. (2008). X chromosome activity in mouse XX primordial germ cells. *PLoS Genet.* 4, e30.
- Creyghton, M.P., Cheng, A.W., Welstead, G.G., Kooistra, T., Carey, B.W., Steine, E.J., Hanna, J., Lodato, M.A., Frampton, G.M., Sharp, P.A., et al. (2010). Histone H3K27ac separates active from poised enhancers and predicts developmental state. *Proc. Natl. Acad. Sci. USA* 107, 21931–21936.
- de Napoles, M., Nesterova, T., and Brockdorff, N. (2007). Early loss of *Xist* RNA expression and inactive X chromosome associated chromatin modification in developing primordial germ cells. *PLoS One* 2, e860.
- Dixon, J.R., Selvaraj, S., Yue, F., Kim, A., Li, Y., Shen, Y., Hu, M., Liu, J.S., and Ren, B. (2012). Topological domains in mammalian genomes identified by analysis of chromatin interactions. *Nature* 485, 376–380.
- Donohoe, M.E., Silva, S.S., Pinter, S.F., Xu, N., and Lee, J.T. (2009). The pluripotency factor Oct4 interacts with Ctf and also controls X-chromosome pairing and counting. *Nature* 460, 128–132.
- Eggan, K., Akutsu, H., Hochedlinger, K., Rideout, W., 3rd, Yanagimachi, R., and Jaenisch, R. (2000). X-Chromosome inactivation in cloned mouse embryos. *Science* 290, 1578–1581.
- Erwin, J.A., del Rosario, B., Payer, B., and Lee, J.T. (2012). An ex vivo model for imprinting: mutually exclusive binding of *Cdx2* and *Oct4* as a switch for imprinted and random X-inactivation. *Genetics* 192, 857–868.
- Gontan, C., Achame, E.M., Demmers, J., Barakat, T.S., Rentmeester, E., van Ijcken, W., Grootegoed, J.A., and Gribnau, J. (2012). RNF12 initiates X-chromosome inactivation by targeting REX1 for degradation. *Nature* 485, 386–390.
- Huynh, K.D., and Lee, J.T. (2003). Inheritance of a pre-inactivated paternal X chromosome in early mouse embryos. *Nature* 426, 857–862.
- Jonkers, I., Monkhorst, K., Rentmeester, E., Grootegoed, J.A., Grosveld, F., and Gribnau, J. (2008). *Xist* RNA is confined to the nuclear territory of the silenced X chromosome throughout the cell cycle. *Mol. Cell. Biol.* 28, 5583–5594.
- Jonkers, I., Barakat, T.S., Achame, E.M., Monkhorst, K., Kenter, A., Rentmeester, E., Grosveld, F., Grootegoed, J.A., and Gribnau, J. (2009). RNF12 is an X-Encoded dose-dependent activator of X chromosome inactivation. *Cell* 139, 999–1011.
- Kalanry, S., Purushothaman, S., Bowen, R.B., Starmer, J., and Magnuson, T. (2009). Evidence of *Xist* RNA-independent initiation of mouse imprinted X-chromosome inactivation. *Nature* 460, 647–651.
- Kay, G.F., Penny, G.D., Patel, D., Ashworth, A., Brockdorff, N., and Rastan, S. (1993). Expression of *Xist* during mouse development suggests a role in the initiation of X chromosome inactivation. *Cell* 72, 171–182.
- Lee, J.T. (2000). Disruption of imprinted X inactivation by parent-of-origin effects at *Tsix*. 103, 17–27.
- Lee, J.T., Davidow, L.S., and Warshawsky, D. (1999). *Tsix*, a gene antisense to *Xist* at the X-inactivation centre. *Nat. Genet.* 21, 400–404.
- Loh, Y.H., Wu, Q., Chew, J.L., Vega, V.B., Zhang, W., Chen, X., Bourque, G., George, J., Leong, B., Liu, J., et al. (2006). The Oct4 and Nanog transcription network regulates pluripotency in mouse embryonic stem cells. *Nat. Genet.* 38, 431–440.
- Luikenhuis, S., Wutz, A., and Jaenisch, R. (2001). Antisense transcription through the *Xist* locus mediates *Tsix* function in embryonic stem cells. *Mol. Cell. Biol.* 21, 8512–8520.
- Ma, Z., Swigut, T., Valouev, A., Rada-Iglesias, A., and Wysocka, J. (2011). Sequence-specific regulator Prdm14 safeguards mouse ESCs from entering extraembryonic endoderm fates. *Nat. Struct. Mol. Biol.* 18, 120–127.
- Maherali, N., Sridharan, R., Xie, W., Utikal, J., Eminli, S., Arnold, K., Stadtfeld, M., Yachechko, R., Tchieu, J., Jaenisch, R., et al. (2007). Directly reprogrammed fibroblasts show global epigenetic remodeling and widespread tissue contribution. *Cell Stem Cell* 1, 55–70.
- Mak, W., Nesterova, T.B., de Napoles, M., Appanah, R., Yamanaka, S., Otte, A.P., and Brockdorff, N. (2004). Reactivation of the paternal X chromosome in early mouse embryos. *Science* 303, 666–669.
- Marahrens, Y., Panning, B., Dausman, J., Strauss, W., and Jaenisch, R. (1997). *Xist*-deficient mice are defective in dosage compensation but not spermatogenesis. *Genes Dev.* 11, 156–166.
- Marahrens, Y., Loring, J., and Jaenisch, R. (1998). Role of the *Xist* gene in X chromosome choosing. *Cell* 92, 657–664.
- Marson, A., Levine, S.S., Cole, M.F., Frampton, G.M., Brambrink, T., Johnstone, S., Guenther, M.G., Johnston, W.K., Wernig, M., Newman, J., et al.

- (2008). Connecting microRNA genes to the core transcriptional regulatory circuitry of embryonic stem cells. *Cell* 134, 521–533.
- Mason, M.J., Plath, K., and Zhou, Q. (2010). Identification of context-dependent motifs by contrasting ChIP binding data. *Bioinformatics* 26, 2826–2832.
- Minkovsky, A., Patel, S., and Plath, K. (2012). Concise review: pluripotency and the transcriptional inactivation of the female Mammalian X chromosome. *Stem Cells* 30, 48–54.
- Namekawa, S.H., Payer, B., Huynh, K.D., Jaenisch, R., and Lee, J.T. (2010). Two-step imprinted X inactivation: repeat versus genic silencing in the mouse. *Mol. Cell. Biol.* 30, 3187–3205.
- Navarro, P., Chambers, I., Karwacki-Neisius, V., Chureau, C., Morey, C., Rougeulle, C., and Avner, P. (2008). Molecular coupling of *Xist* regulation and pluripotency. *Science* 321, 1693–1695.
- Navarro, P., Oldfield, A., Legoupi, J., Festuccia, N., Dubois, A., Attia, M., Schoorlemmer, J., Rougeulle, C., Chambers, I., and Avner, P. (2010). Molecular coupling of *Tsix* expression and pluripotency. *Nature* 468, 457–460.
- Navarro, P., Moffat, M., Mullin, N.P., and Chambers, I. (2011). The X-inactivation trans-activator *Rnf12* is negatively regulated by pluripotency factors in embryonic stem cells. *Hum. Genet.* 130, 255–264.
- Nesterova, T.B., Senner, C.E., Schneider, J., Alcayna-Stevens, T., Tattermusch, A., Hemberger, M., and Brockdorff, N. (2011). Pluripotency factor binding and *Tsix* expression act synergistically to repress *Xist* in undifferentiated embryonic stem cells. *Epigenetics Chromatin* 4, 17.
- Niwa, H., Miyazaki, J., and Smith, A.G. (2000). Quantitative expression of *Oct-3/4* defines differentiation, dedifferentiation or self-renewal of ES cells. *Nat. Genet.* 24, 372–376.
- Nora, E.P., Lajoie, B.R., Schulz, E.G., Giorgetti, L., Okamoto, I., Servant, N., Piolot, T., van Berkum, N.L., Meisig, J., Sedat, J., et al. (2012). Spatial partitioning of the regulatory landscape of the X-inactivation centre. *Nature* 485, 381–385.
- Okamoto, I., Otte, A.P., Allis, C.D., Reinberg, D., and Heard, E. (2004). Epigenetic dynamics of imprinted X inactivation during early mouse development. *Science* 303, 644–649.
- Patrat, C., Okamoto, I., Diabanguaya, P., Vialon, V., Le Baccon, P., Chow, J., and Heard, E. (2009). Dynamic changes in paternal X-chromosome activity during imprinted X-chromosome inactivation in mice. *Proc. Natl. Acad. Sci. USA* 106, 5198–5203.
- Penny, G.D., Kay, G.F., Sheardown, S.A., Rastan, S., and Brockdorff, N. (1996). Requirement for *Xist* in X chromosome inactivation. *Nature* 379, 131–137.
- Plath, K., Fang, J., Mlynarczyk-Evans, S.K., Cao, R., Worringer, K.A., Wang, H., de la Cruz, C.C., Otte, A.P., Panning, B., and Zhang, Y. (2003). Role of histone H3 lysine 27 methylation in X inactivation. *Science* 300, 131–135.
- Raj, A., van den Bogaard, P., Rifkin, S.A., van Oudenaarden, A., and Tyagi, S. (2008). Imaging individual mRNA molecules using multiple singly labeled probes. *Nat. Methods* 5, 877–879.
- Rastan, S., and Robertson, E.J. (1985). X-chromosome deletions in embryo-derived (EK) cell lines associated with lack of X-chromosome inactivation. *J. Embryol. Exp. Morphol.* 90, 379–388.
- Reményi, A., Lins, K., Nissen, L.J., Reinbold, R., Schöler, H.R., and Wilmanns, M. (2003). Crystal structure of a POU/HMG/DNA ternary complex suggests differential assembly of *Oct4* and *Sox2* on two enhancers. *Genes Dev.* 17, 2048–2059.
- Sado, T., Wang, Z., Sasaki, H., and Li, E. (2001). Regulation of imprinted X-chromosome inactivation in mice by *Tsix*. *Development* 128, 1275–1286.
- Sado, T., Li, E., and Sasaki, H. (2002). Effect of *TSIX* disruption on *XIST* expression in male ES cells. *Cytogenet. Genome Res.* 99, 115–118.
- Silva, J., Mak, W., Zvetkova, I., Appanah, R., Nesterova, T.B., Webster, Z., Peters, A.H.F.M., Jenuwein, T., Otte, A.P., and Brockdorff, N. (2003). Establishment of histone h3 methylation on the inactive X chromosome requires transient recruitment of *Eed-Enx1* polycomb group complexes. *Dev. Cell* 4, 481–495.
- Silva, J., Nichols, J., Theunissen, T.W., Guo, G., van Oosten, A.L., Barrandon, O., Wray, J., Yamanaka, S., Chambers, I., and Smith, A. (2009). *Nanog* is the gateway to the pluripotent ground state. *Cell* 138, 722–737.
- Stadtfeld, M., Maherali, N., Breault, D.T., and Hochedlinger, K. (2008). Defining molecular cornerstones during fibroblast to iPS cell reprogramming in mouse. *Cell Stem Cell* 2, 230–240.
- Sugimoto, M., and Abe, K. (2007). X chromosome reactivation initiates in nascent primordial germ cells in mice. *PLoS Genet.* 3, e116.
- Tada, M., Takahama, Y., Abe, K., Nakatsuji, N., and Tada, T. (2001). Nuclear reprogramming of somatic cells by in vitro hybridization with ES cells. *Curr. Biol.* 11, 1553–1558.
- Tchieu, J., Kuoy, E., Chin, M.H., Trinh, H., Patterson, M., Sherman, S.P., Aimiwu, O., Lindgren, A., Hakimian, S., Zack, J.A., et al. (2010). Female human iPSCs retain an inactive X chromosome. *7*, 329–342.
- Tsai, C.L., Rowntree, R.K., Cohen, D.E., and Lee, J.T. (2008). Higher order chromatin structure at the X-inactivation center via looping DNA. *Dev. Biol.* 319, 416–425.
- Tucker, K.L., Wang, Y., Dausman, J., and Jaenisch, R. (1997). A transgenic mouse strain expressing four drug-selectable marker genes. *Nucleic Acids Res.* 25, 3745–3746.
- van den Berg, D.L.C., Zhang, W., Yates, A., Engelen, E., Takacs, K., Bezstarosti, K., Demmers, J., Chambers, I., and Poot, R.A. (2008). Estrogen-related receptor beta interacts with *Oct4* to positively regulate *Nanog* gene expression. *Mol. Cell. Biol.* 28, 5986–5995.
- Williams, L.H., Kalantry, S., Starmer, J., and Magnuson, T. (2011). Transcription precedes loss of *Xist* coating and depletion of H3K27me3 during X-chromosome reprogramming in the mouse inner cell mass. *Development* 138, 2049–2057.
- Wutz, A., and Jaenisch, R. (2000). A shift from reversible to irreversible X inactivation is triggered during ES cell differentiation. *Mol. Cell* 5, 695–705.